Supplementary S2

Background

Encompassed below are the additional methods to determine the horizontal and vertical areas covered by the overlapping fields of view. Expressly, the area where birds are visible by all three cameras and their flight height can be triangulated and measured. We calculated maximum measurable heights and determined the effect of varying configuration: distances between configurations and the structure/object of interest (OoI), spacing between cameras of the configuration, and whether the configuration was horizontally angled. The calculation of these supplementary details was prompted by inquiry regarding the area and height limitations of this stereophotogrammetric approach.

Methods and Materials

Calculating angles of view

Camera angles of view (α_h; α_w) were calculated separately for the sensor height (s_h) and width (s_w) of the Canon 1300D used at 55 mm focal length (f) (Eq. S1; Fig. S2).

$$\alpha_{h,w} = \tan^{-1}\frac{s_h, s_w}{2f} \quad \text{(Eq. S1.1)}$$

$$\alpha_h = 0.269\,rad,\ \alpha_w = 0.4\,rad \quad \text{(Eq. S1.2)}$$

$$\alpha_h = 15.428°,\ \alpha_w = 22.918° \quad \text{(Eq. S1.3)}$$

Top view

Given the angles of view for the three similar cameras from a top view (α_w), we set out to calculate the area of horizontal overlap between the three cameras, where bird flight height

could be measured. By varying camera configurations and their associated dimensions, we could determine their effect on the area of overlap (Fig. S3). We varied the distance (d_o) to the object of interest (OoI, to which the cameras were pointed), straight distances between the cameras (x_w), and whether the camera configuration was angled or not, which decided whether this straight distance (x_w) was the actual distance (x_{wa}) between the cameras (Eq. S2)

$$\text{If angled } (\delta = 26.565°) \text{ configuration: } x_{wa} = \sqrt{x_w^2 + (\frac{x_w}{2})^2} \qquad \text{(Eq. S2.1)}$$

$$\text{If straight configuration } (\delta = 0°): x_{wa} = x_w \qquad \text{(Eq. S2.2)}$$

From the actual distance between the cameras, we determined both outer cameras' approximate distances to the centre of the plane representing the object of interest (b; Eq. S3).

$$b = \sqrt{d_o^2 + x_{wa}^2 - 2d_o x_{wa} \times \sin\delta} \qquad \text{(Eq. S3)}$$

Using the known distances between the outer cameras (b) and the central camera (d_o) to the centre of the object plane of interest, we calculated the inward rotation required for the principal components of the outer cameras to intersect the centre of the object of interest (r_w; Eq. S4).

$$r_w = \cos^{-1}(\frac{b^2 + d_o^2 - x_{wa}^2}{2bd_o}) \qquad \text{(Eq. S4)}$$

We then determined the angle at the point where all three fields of view overlap (α_{w3}; Eq. S5), comprising the rotations of the outer fields of view.

$$\alpha_{w3} = \alpha_w + 2r_w \qquad \text{(Eq. S5)}$$

Assuming that the outer camera angles were similarly spaced from the central camera and are similarly rotated inwards, we also assumed that overlapping area was an isosceles triangle. The base of this triangle was the width of the overlapping fields of view at the object of interest (w_o). It was calculated from the camera angle of view (α_w) and the distance between the central camera and the object of interest (d_o; Eq. S6).

$$w_o = \frac{\sin\frac{\alpha_w}{2} \times d_o}{\cos\frac{\alpha_w}{2}} \times 2 \quad \text{(Eq. S6)}$$

The triangular height of this area was the distance from the first point of overlap to the object of interest (d_{w3}; Eq. S7).

$$d_{w3} = \frac{\cos(\frac{\alpha_{w3}}{2}) \times \frac{w_o}{2}}{\sin(\frac{\alpha_{w3}}{2})} \quad \text{(Eq. S7)}$$

To calculate the area extending behind the OoI, we required the additional distance considered behind the object of interest (d_a) and the angle for the area with overlapping fields of view behind the object (β; Eq. S8).

$$\beta = (90° - r_w) + \frac{\alpha_w}{2} \quad \text{(Eq. S8)}$$

Thereafter, we could calculate the horizontal area covered by the overlapping fields of view, within which we could estimate the flight height of birds.

Horizontal Surface Area

There were two components to the horizontal area coverage calculation (Fig. S3):

(1) The area after which all three fields of view began to overlap, but before they intersected at the object of interest. It was assumed that this intersection is complete, based on all three cameras perfectly pointing at the centre of the object of interest. This area (SA_{t1}) was calculated using a simple triangle area calculation with the distance point of first overlap to the object of interest (d_{w3}) and the width of intersecting fields of view at the object of interest (w_o; Eq. S9).

$$SA_{t1} = \frac{w_o \times d_{w3}}{2} \quad \text{(Eq. S9)}$$

(2) The area after the fields of view intersected with each other at the object of interest. Depending on the degree of rotation inwards by the outer cameras this area could continue indefinitely or taper. If the outer camera's rotation inwards (r_w) was greater than half the angle of view (α_w), then the field of view tapered (first case). Otherwise, rotation was equal to or less than half the angle of view, and the field of view continued indefinitely, at a constant or increasing width (second case). Regardless, the additional length of this component was dictated (d_a) and depended on the size of the bird in the field of view, visibility that day, obstructions, etc. Firstly, a rectangular area was calculated based on the additional distance considered past the object of interest and the width of the intersecting fields of view at the object of interest. Thereafter, additional angular components were subtracted (first case) or added (second case) to the rectangular area (Eq. S10).

$$\text{If } r_w > \frac{\alpha_w}{2}\text{: } SA_{t2} = (d_a \times w_o) + \frac{(\frac{\sin(\beta - 90°) \times d_a}{\cos(\beta - 90°)}) \times d_a}{2} \quad \text{(Eq. S10.1)}$$

$$\text{If } r_w \leq \frac{\alpha_w}{2}\text{: } SA_{t2} = (d_a \times w_o) - \frac{(\frac{\sin(|\beta - 90°|) \times d_a}{\cos(|\beta - 90°|)}) \times d_a}{2} \quad \text{(Eq. S10.2)}$$

Thereafter, the two components of the top surface area were added to indicate the horizontal area in which bird flight height could be measured (Eq. S11).

$$SA_t = SA_{t1} + SA_{t2} \quad \text{(Eq. S11)}$$

The accuracy of this measurement varied with distance as illustrated in the main typescript. Inputting variable camera configurations, distances between cameras, distance to the object of interest, and acceptable additional distances behind the object of interest, we were able to calculate and compare the horizontal area covered by each variation of the camera configuration.

Side view

Given the angles of view for the three similar cameras from a side view (α_h), we calculated the area of vertical overlap between the three cameras, where bird flight height could be measured. We also determined how adjusting the camera configuration affected this area of overlap (Fig. S4). We had input variables for the distance (d_o) to the object of interest (OoI). The vertical heights for the cameras remained constant, with the central camera positioned 0.5 m (z_{h1}) off the ground on a tripod and the outer cameras positioned 1.8 m (z_h; $z_{h2} = 1.3\ m$, or the vertical distance between the two cameras) off the ground on tripods (Eq. S12).

$$z_h = z_{h1} + z_{h2} = 1.8\ m \quad \text{(Eq. S12)}$$

Cameras were rotated to sufficiently cover the ground and have the OoI in the full field of view where both cameras are assumed to intersect perfectly. As with the real case, it is assumed that the ground plane can be extrapolated. The cameras were not vertically rotated similarly, the central camera is rotated upwards (r_{h1}) more than the outer cameras (r_{h2}). Ideally,

one should maximise the upwards rotation to get a better field of view above the ground. However, a maximum rotation upwards (r_{h1max} for the lower central camera and r_{h2max} for the higher outer cameras) was set based on at least some intersection approximately 2 m from the OoI. This was to allow for sufficient ground surface to place landmarks. The maximum rotation upwards thus depended on the distance of the outer and inner cameras from the OoI. For leeway, we arbitrarily subtracted 0.5° (Eq. S13).

$$r_{h1max} = \frac{\alpha_h}{2} - \cos^{-1}\left(\frac{\sqrt{(d_o-2)^2+z_{h1}^2}^2 + (d_o-2)^2 - z_{h1}^2}{2\times\left(\sqrt{(d_o-2)^2+z_{h1}^2}\right)\times(d_o-2)}\right) - 0.5° \qquad \text{(Eq. S13.1)}$$

$$r_{h2max} = \frac{\alpha_h}{2} - \cos^{-1}\left(\frac{\sqrt{(d_o-2)^2+z_h^2}^2 + (d_o-2)^2 - z_h^2}{2\times\left(\sqrt{(d_o-2)^2+z_h^2}\right)\times(d_o-2)}\right) - 0.5° \qquad \text{(Eq. S13.2)}$$

For an OoI 10 m away, $r_{h1max} = 3.63°$ upwards, $r_{h2max} = -5.47°$ upwards. For an OoI 100 m away, $r_{h1max} = 6.92°$ upwards, $r_{h2max} = 6.16°$ upwards. For an OoI 200 m away, $r_{h1max} = 7.07°$ upwards, $r_{h2max} = 6.69°$ upwards. This meant that the further the cameras were away from the OoI, the cameras and thus their fields of view could potentially be angled further upwards, improving the heights at which birds could be measured. We thus assumed that the camera angles were optimised for estimating bird flight height (Eq. S14).

$$r_{h1} = r_{h1max} \qquad \text{(Eq. S14.1)}$$

$$r_{h2} = r_{h2max} \qquad \text{(Eq. S14.2)}$$

For angled configurations, the calculations for r_{h1max} and r_{h2max} used different d_o values, adjusted for the distances the outer cameras are moved forward. Once all factors associated with horizontal rotation of the cameras were accounted for, we calculated the relative angular

difference between these two rotations (Δr_h; Eq. S15) and the average rotation for the inner and outer cameras ($\bar{r_h}$; Eq. S15).

$$\Delta r_h = r_{h1} - r_{h2} \quad \text{(Eq. S15)}$$

$$\bar{r_h} = \frac{r_{h1}+r_{h2}}{2} \quad \text{(Eq. S15)}$$

The angle between the intersecting fields of view (α_{h3}; Eq. S16) was dependent on the camera angles of view (α_h) and the relative rotation of the cameras to each other (Δr_h).

$$\alpha_{h3} = \alpha_h + \Delta r_h \quad \text{(Eq. S16)}$$

We then calculated the dimensions of the triangle representing the overlapping fields of view before they intersected at 2 m before the OoI (Eq. S17).

$$c = \frac{\sin\left(\left(90+\frac{\alpha_h}{2}\right)+r_{h2}\right)\times z_{h2}}{\sin\left(180-\left(\left(90+\frac{\alpha_h}{2}\right)+r_{h2}\right)-\left(\left(90-\frac{\alpha_h}{2}\right)-r_{h1}\right)\right)} - \left(\frac{\sin\left(\left(90-\frac{\alpha_h}{2}\right)+r_{h2}\right)\times z_{h2}}{\sin(\alpha_{h3})}\right) \quad \text{(Eq. S17.1)}$$

$$b = \sqrt{(d_o-2)^2 + z_h} - \left(\frac{\sin\left(\left(90-\frac{\alpha_h}{2}\right)-r_{h1}\right)\times z_{h2}}{\sin(\alpha_{h3})}\right) \quad \text{(Eq. S17.2)}$$

$$h_i = \sqrt{b^2 + c^2 - 2bc\cos\alpha_{h3}} \quad \text{(Eq. S17.3)}$$

Thereafter, we calculated the dimensions for the triangular area just behind the area of intersecting fields of view, 2 m in front of the OoI (Eq. S18).

$$s = \frac{\sin(\bar{r_h})\times h_i}{\sin\left(\left(90-\frac{\alpha_h}{2}\right)-r_{h2}\right)} \quad \text{(Eq. S18.1)}$$

$$h_h = \frac{\sin(180-(\bar{r_h}+\left(90-\frac{\alpha_h}{2}\right))\times h_i}{\sin(\left(90-\frac{\alpha_h}{2}\right)-r_{h2})} \quad \text{(Eq. S18.2)}$$

We formulated the additional angular height above the rectangle with distance (Eq. S19).

$$t = d_a\tan(\frac{\alpha_h}{2} + r_{h2}) \quad \text{(Eq. S19)}$$

Vertical Surface Area

After preparing the dimensions, we calculated the area coverage. Again, the total area coverage was divided into two components.

(1) The overlapping fields of view before perfect intersection 2 m in front of the camera. The area for overlapping fields of view until the point of intersection was calculated using Heron's formula. We also included the area coverage up until the OoI (SA_{s1}; Eq. S20).

$$p = \frac{b+c+h_i}{2} \quad \text{(Eq. S20.1)}$$

$$SA_{s1} = \sqrt{p(p-b)(p-c)(p-h_i)} + \frac{4\tan(\frac{\alpha_h}{2}+r_{h2})}{2} + 2h_h \quad \text{(Eq. S20.2)}$$

(2) The overlapping fields of view behind the OoI consisted of a rectangular component and a continued triangular component. The camera heights of 1.8 m in our configuration are unlikely to be higher than any OoI, and as such, this area was assumed to only increase with distance. This component was calculated as follows (Eq. S21):

$$SA_{s2} = d_a(h_h + 2) + \frac{d_a\tan(\frac{\alpha_h}{2}+r_{h2})}{2} \quad \text{(Eq. S21)}$$

These two components were added up to determine the total vertical coverage by the camera configuration (SA_s; Eq. S22).

$$SA_s = SA_1 + SA_2 \quad \text{(Eq. S22)}$$

Height

The point of interest, to be measured for height above ground needed to occur somewhere within the overlapping fields of view. We calculated how far this point is in front of or behind the vertical point of first intersection (d_3; Eq. S23).

$$d_{w3c} = d_o - d_{w3} \quad \text{(Eq. S23.1)}$$

$$d_{h3c} = \tan\left(\left(90 - \frac{\alpha_h}{2}\right) + r_{h2}\right) \times \frac{z_{h2}}{2} \quad \text{(Eq. S23.2)}$$

$$\text{If } d_{w3c} < d_{h3c}\text{: } d_3 = d_{w3c} \quad \text{(Eq. S23.3)}$$

$$\text{If } d_{w3c} > d_{h3c}\text{: } d_3 = d_{h3c} \quad \text{(Eq. S23.4)}$$

One approach was used to calculate the maximum heights up until the vertical fields of view intersected perfectly (d_{h3p}; Eq. S25).

$$d_{h3p} = d_o - \sin(\bar{r_h}) \times h_i \quad \text{(Eq. S24)}$$

We determined where fields of view began to taper horizontally (d_{tap}; Eq. S25).

$$\text{If } \beta < 90\text{: } d_{tap} = w_o \tan(\beta) \quad \text{(Eq. S25)}$$

Thereafter, another approach is used to calculate the maximum height. The distance from the camera where one wants to measure the height is d. Height can only be calculated for d_3 onwards (Eq. S26).

Where $d < d_3$: Height cannot be measured. (Eq. S26.1)

Where $d > d_3$ & $d < d_{h3p}$: $H_{max} = z_{h1} + \tan(\frac{\alpha_h}{2} + r_{h1}) \times (d - d_3)$ (Eq. S26.2)

Where $d > d_{h3p}$: $H_{max} = z_h + \tan(\frac{\alpha_h}{2} + r_{h2}) \times (d - d_3)$ (Eq. S26.3)

Where $d < (d_o + d_{tap})$: Height cannot be measured. (Eq. S26.4)

Statistical Analyses

Using the horizontal (top-down) and vertical (side-view) formulae in Excel (Microsoft ©), we superficially compared projects from 10 to 180 m away from the object of interest, with distances between cameras of 5, 10, 20 m, at either a straight ($\delta = 0°$) or an angled configuration ($\delta = 26.565°$). For each project, we calculated the horizontal (SA_t) and vertical (SA_s) area covered and recorded the area increase or decrease after the object of interest. When calculating the maximum height between the configurations, we assumed that all the configurations were 100 m away from the OoI. We calculated and compared the change in the maximum measurable height up to 200 m away from the cameras, i.e., 100 m behind and in front of the OoI.

Results

All projects with distances 10 m away from the object of interest were problematic in that their additional area of horizontal coverage decreased soon after the object of interest at a rate of 0.15 to 2.98 $m^2.m^{-1}$ (Fig. S5) with starting coverages of 1.08 to 3.90 m^2 directly (1 m) behind

the object of interest. At 10 m away, the horizontal area covered behind the object of interest tapered off within 2-7 m. While including the area in front of the object of interest, this totalled 12-17 m overlapping distance and an area of 6.33 to 10.60 m^2 covered by the cameras. This only includes projects that worked despite the extreme proximity of cameras to the OoI and tapering fields of view thereafter. Some projects were too close to have intersecting fields of view on the object of interest: e.g., cameras 10 m away, in an angled configuration, with ≥ 10 m between them. The further the cameras were away from the object of interest, the less the cameras needed to be rotated inwards towards the object of interest and the higher the rate of increase (0.11 to 0.18 $m^2.m^{-1}$) for the additional area behind the object of interest.

Angled configurations attained higher horizontal area coverages than straight configurations when the distance from the object of interest was high, > 90 m with 20 m between cameras, > 45 m with 10 m between cameras, > 27 m with 5 m between cameras (Fig. S6). At distances lower than this, the straight configuration attained larger coverage. The horizontal spacing between the cameras affected the minimum distance in front of the cameras at which bird flight height can be measured. Angled cameras allow bird flight height to be measured closer to the central camera at greater distances from the vertical structure of interest (Fig. S7).

For straight configurations, the vertical area increased at a higher rate after the OoI with distances from the OoI, outperforming angled configurations, (Fig. S8). The straight configurations also attained slightly higher vertical areas of coverages at more than 40 m away from the OoI (Fig. S9). However, when taking the top-down point of first intersection into account when calculating the maximum measurable height, the angled configuration slightly outperformed the straight configurations, this benefit increased with increased distance

between the camera and the OoI (Fig S10). At 150 m away from the OoI, the angled configuration spaced ~5 m wide was able to measure the highest flight heights. When measuring height, the configurations 10-50 m away performed the worst, thereafter, the maximum measurable flight height seemed to be optimised where the cameras were 90-100 m away from the OoI for configurations spaced 10 – 20 m apart (Fig. S11) but continued to increase with configurations that were spaced 5 m apart (Fig. S12).

Discussion

Using the sets of 2-D trigonometric calculations (top-down and side-view), we briefly illustrate the interaction between the increased distances from the focal structures (object of interest; OoI) with increased area of the overlapping fields of view, horizontally and vertically, especially if the cameras are correctly positioned and orientated. Generally, the trend is for the vertical area to increase if cameras are far enough from the focal object of interest, to which the cameras are pointed. Too close, and the fields of view from the spatially separated cameras start to wrap around the focal object and the overlapping field of view tapers behind the object of interest.

Herein, we assume that the OoI did not cast a shadow in the overlapping fields of view that would subtract from the second component of the area of coverage. We also simplified the interaction between the horizontal and vertical area coverage and did not produce a complex 3-D volume over overlapping fields of view. However, we believe the horizontal and vertical surfaces coverages provide a sufficient starting point to determine the general area covered by various versions of our camera configurations.

Figures

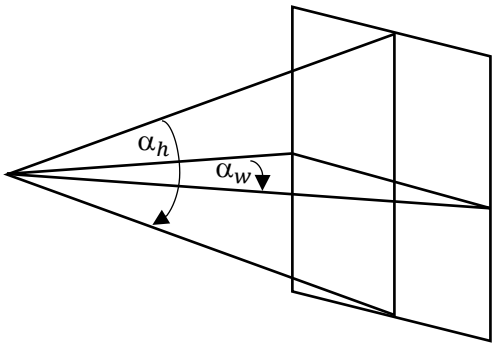

Fig. S2. Maximum ranges of images radiating out from a central camera onto a plane of photographic interest. The camera angles of view are illustrated for height (α_h) and width (α_w).

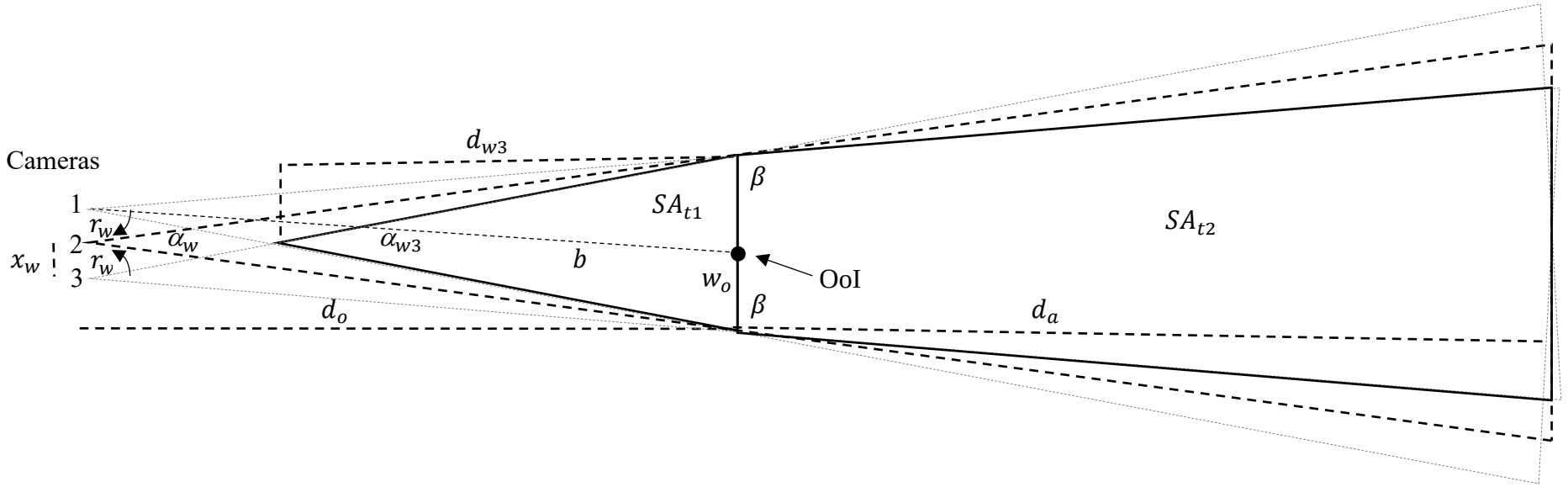

Fig. S3. A top-down geometric visualisation to calculate the total horizontal area of overlapping fields of view (coverage; solid black) between the three cameras. The central camera's field of view (dashed triangles) is distinguished from the outer cameras (dotted triangles). The overlapping fields of view consist of 2 parts: the triangle before the object of interest (OoI) and the quadrilateral behind the OoI, with a variable length of additional distance (d_a). The known variables are the horizontal angle of view (α_w), the distance from the central camera to the OoI (d_o) and the distances between the cameras (x_w). The rest of the variables are unknown and derive from the calculations with the known variables to ultimately determine the surface area and volumes for the overlapping fields of view, where bird flight heights can be photogrammetrically measured.

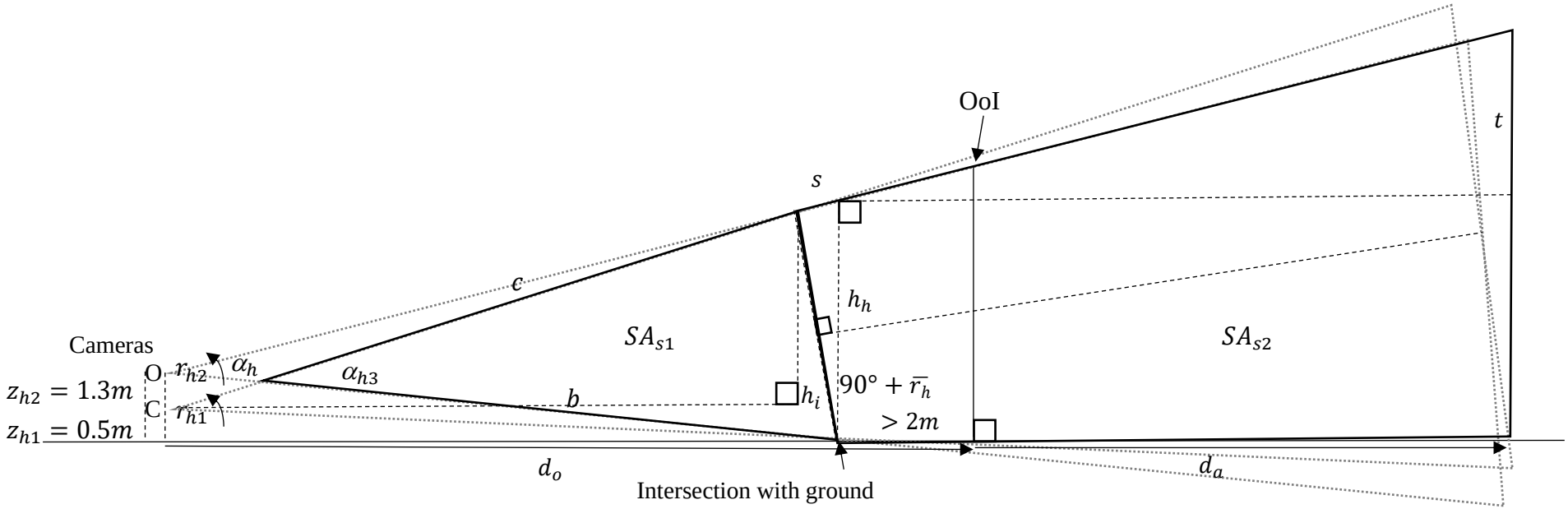

Fig. S4. The side-view geometric visualisation to calculate the total vertical area of overlapping fields of view (coverage; solid black) between the three cameras. It consists of 2 parts: the triangle 2 m before the object of interest (OoI), which will include the area until the OoI in the area calculation (SA_{s1}), and the quadrilateral behind the OoI, with a variable additional distance (d_a). The known variables are the vertical angle of view (α_h), the horizontal distance from the central camera to the top of the OoI (d_o) and the vertical distances between the cameras and the ground (z_{h1} & z_{h2}). The ground plane is also illustrated as a solid black line. The rest of the variables are unknown and derived from the calculations with the known variables to ultimately determine the surface area for the overlapping fields of view, where bird flight heights can be photogrammetrically measured.

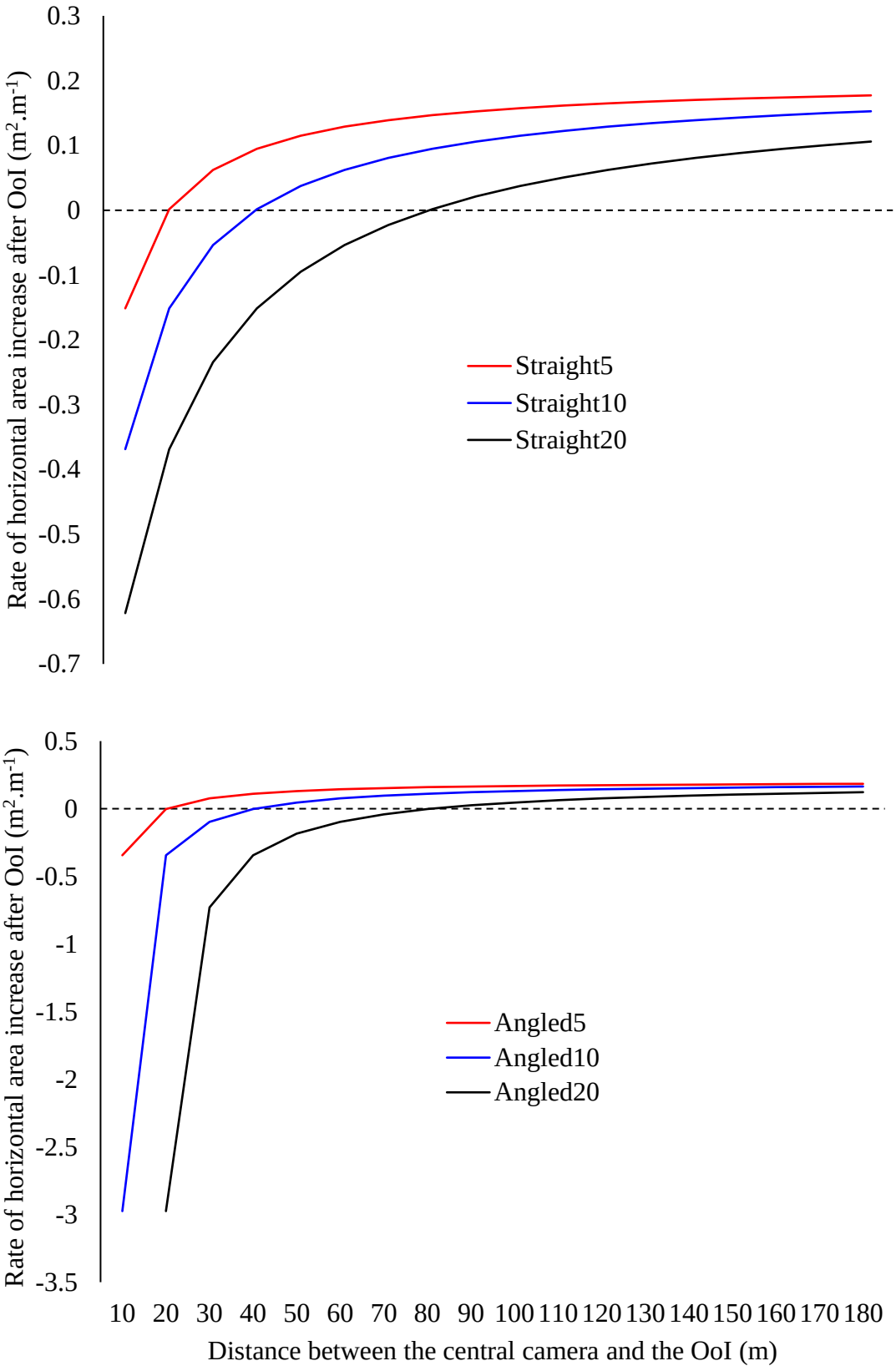

Fig. S5. We compare the rate of horizontal area coverage increase ($m^2.m^{-1}$) after the object of interest (OoI) with increasing distance between the cameras and the OoI (m).

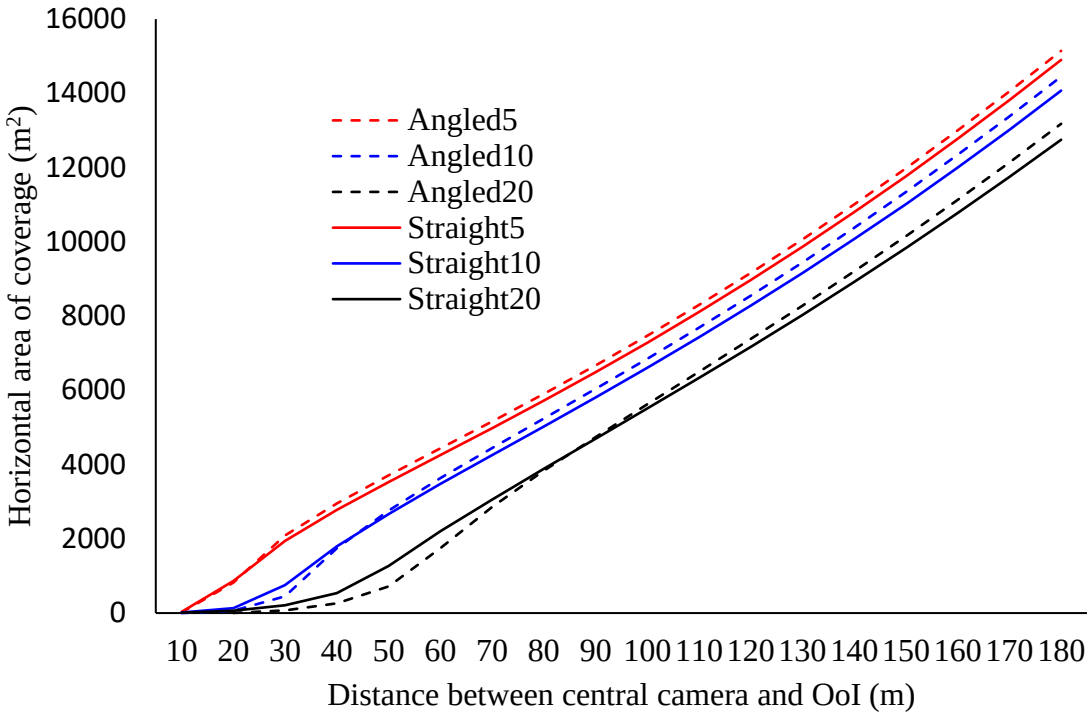

Fig. S6. Including a potential 100 m behind the object of interest (OoI), we illustrate the relationship between the total horizontal area of coverage (m^2), with increasing distance between the cameras and the object of interest.

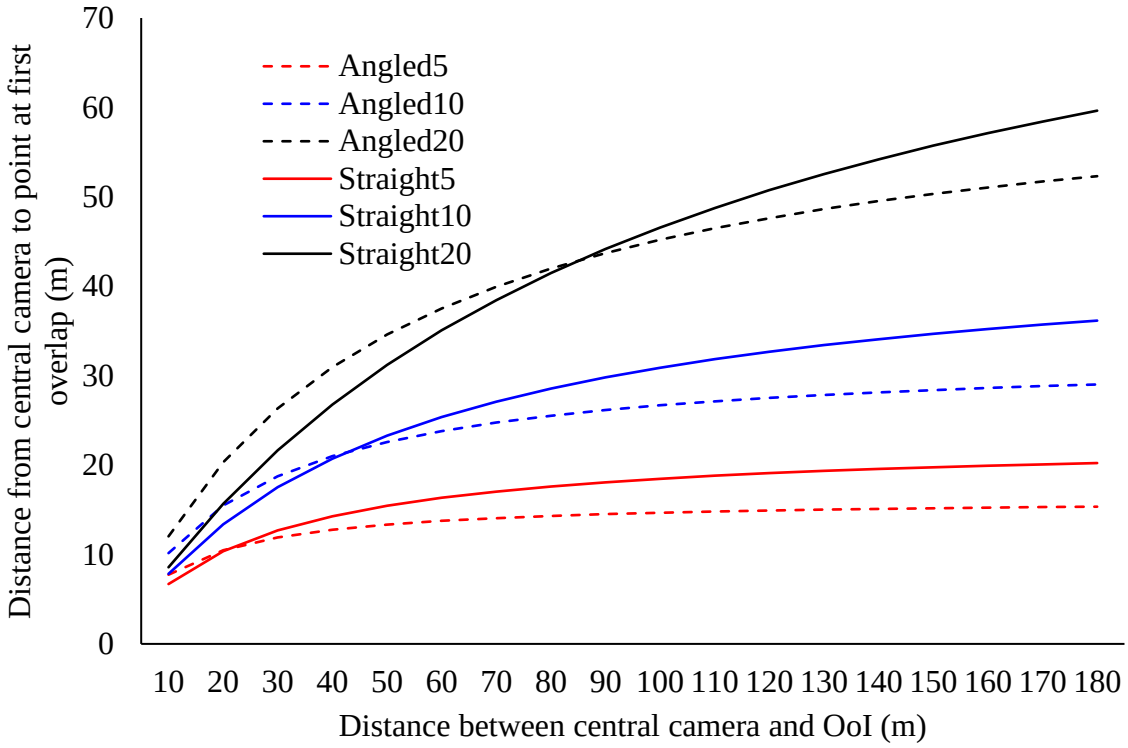

Fig. S7. The distance (m) in front of the central camera where all three fields of view begin to overlap, with increasing distances between the camera and the object of interest (OoI).

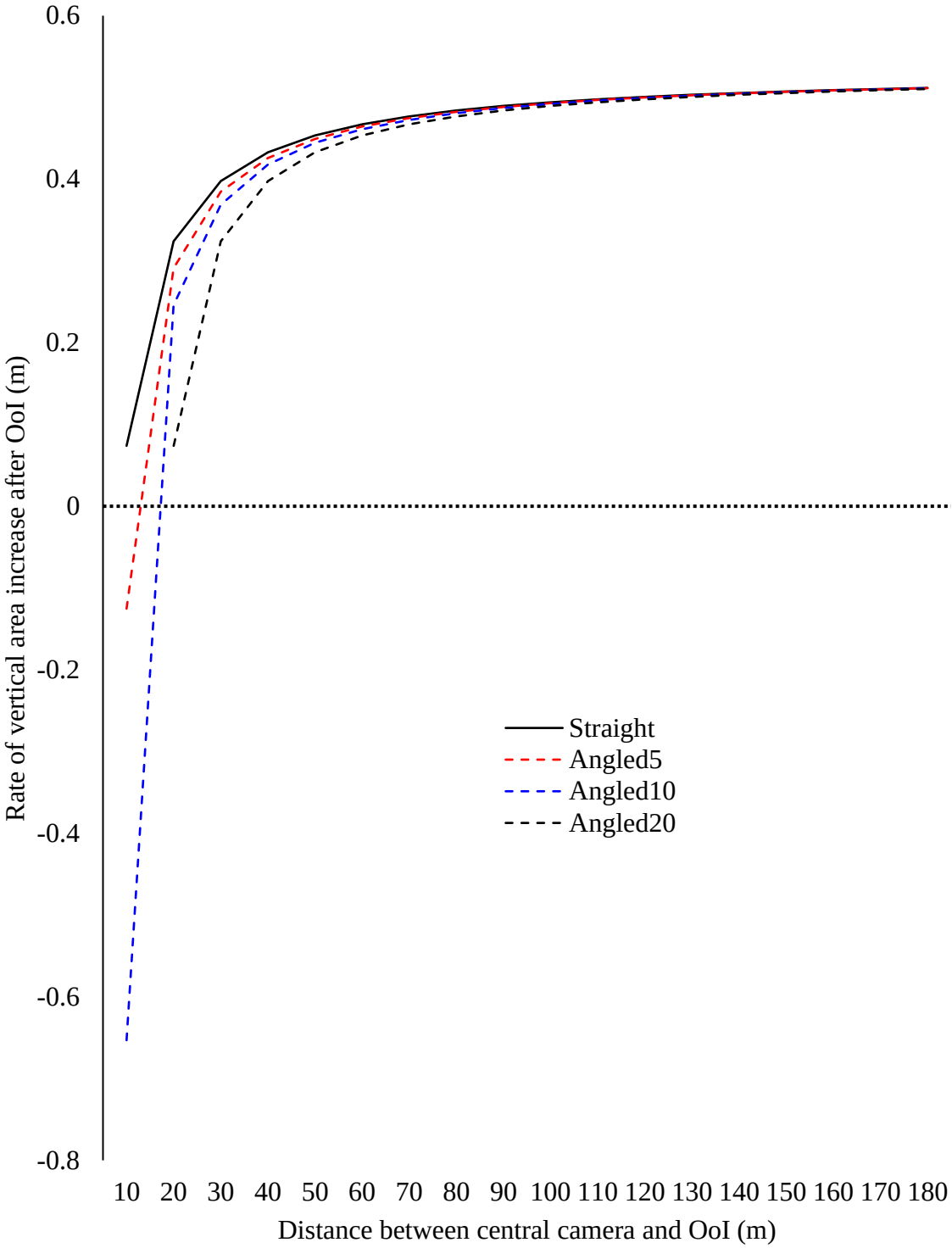

Fig. S8. We compare the rate of vertical area coverage increase ($m^2.m^{-1}$) after the object of interest (OoI) with increasing distance between the cameras and the OoI (m). As there is no difference between the straight configurations from a side-view, they were lumped together.

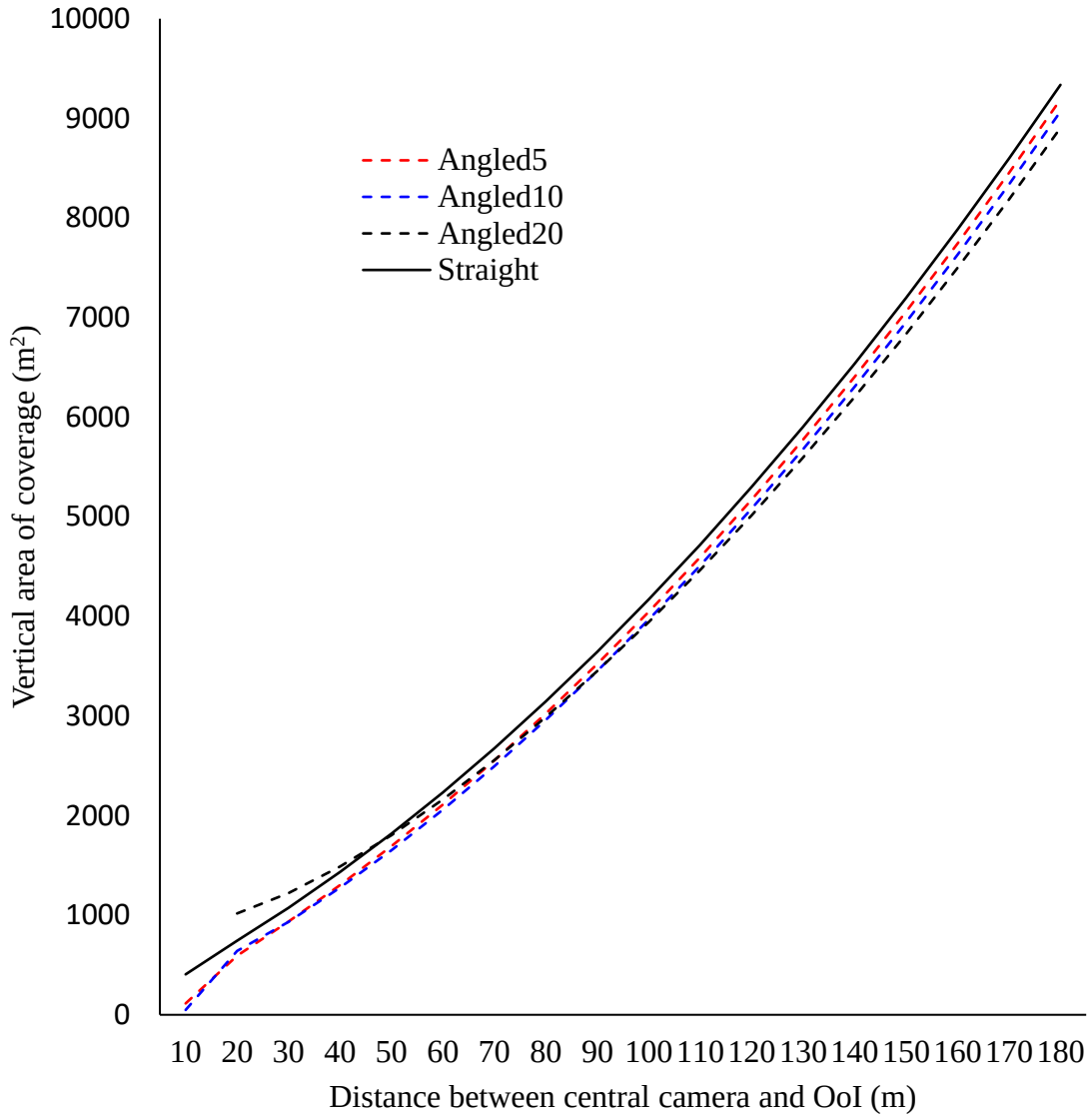

Fig. S9. Including a potential 100 m behind the object of interest (OoI), we illustrate the relationship between the total vertical area of coverage (m^2), with increasing distance between the cameras and the object of interest. As there is no difference between the straight configurations from a side-view, they were lumped together.

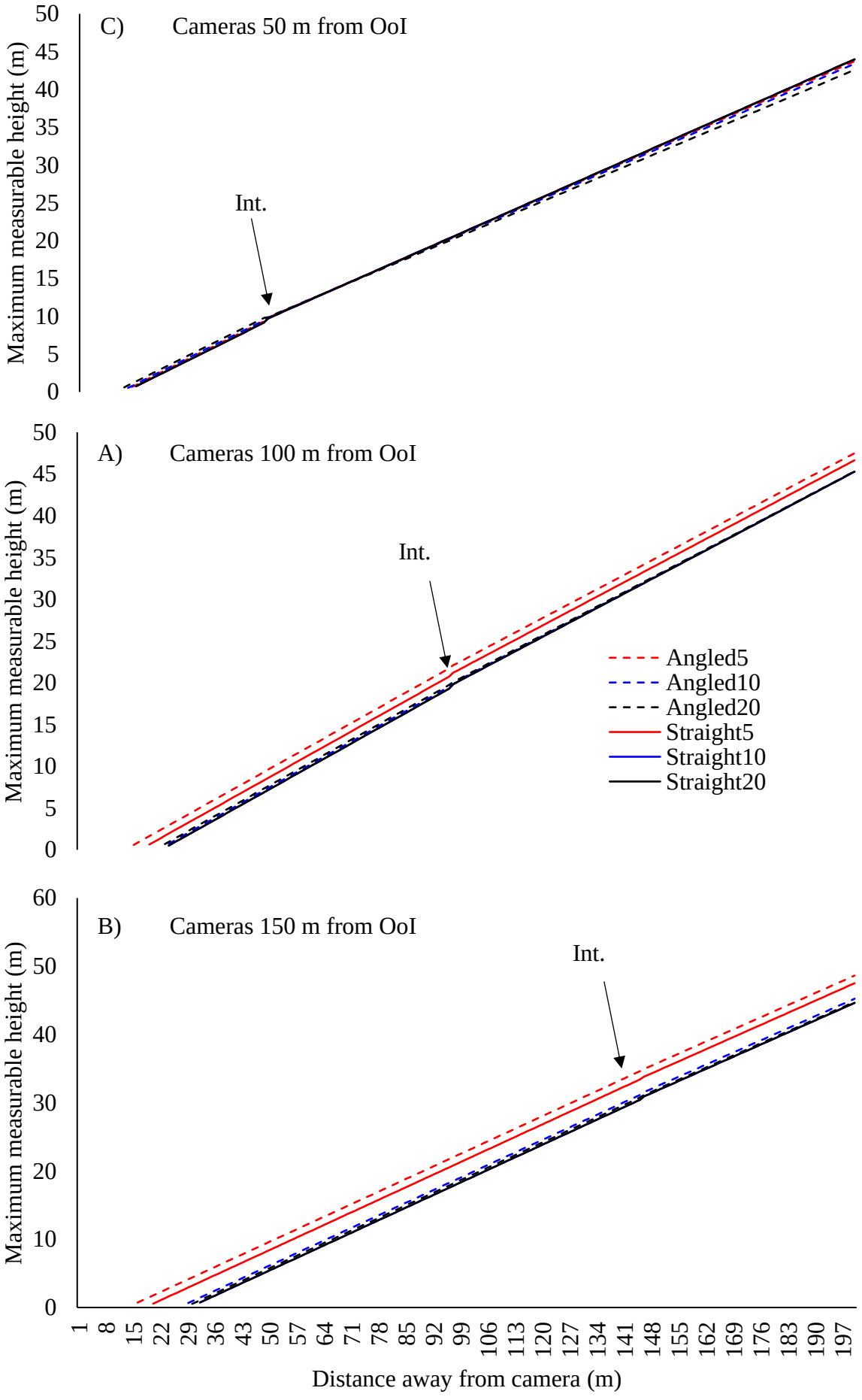
C)
Cameras 50 m from OoI
Int.
Maximum measurable height (m)
A)
Cameras 100 m from OoI
Int.
Angled5
Angled10
Angled20
Straight5
Straight10
Straight20
B)
Cameras 150 m from OoI
Int.
Distance away from camera (m)

Fig. S10. The maximum measurable heights for all camera configurations with distance away from the camera at 50 m, 100 m, and 150 m between the camera and the OoI, respectively. The slight change in direction in the relationship occurs where the fields of view perfectly intersect (Int.).

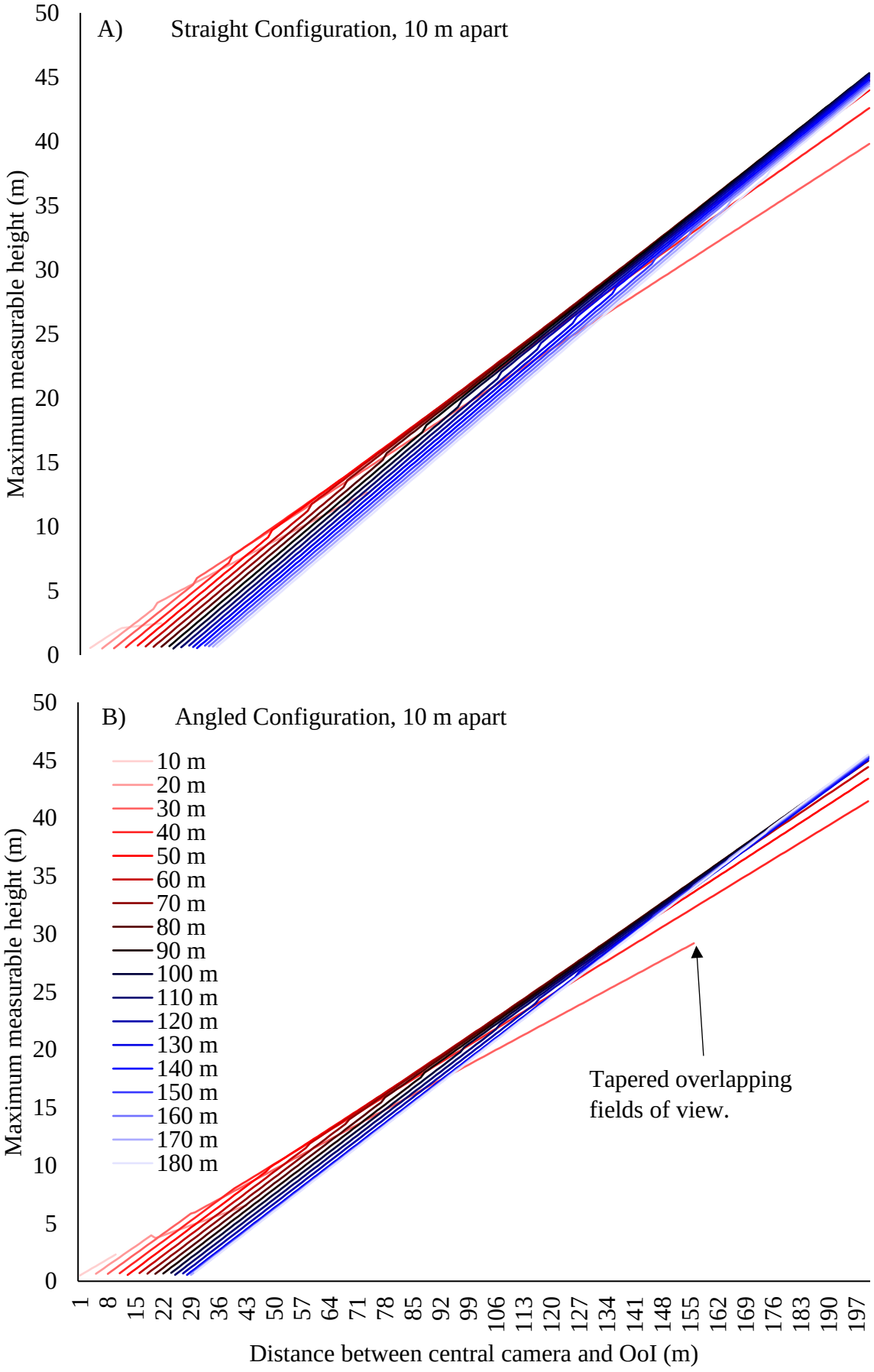
A)
Straight Configuration, 10 m apart
Maximum measurable height (m)
0
5
10
15
20
25
30
35
40
45
50
B)
Angled Configuration, 10 m apart
10 m
20 m
30 m
40 m
50 m
60 m
70 m
80 m
90 m
100 m
110 m
120 m
130 m
140 m
150 m
160 m
170 m
180 m
Tapered overlapping fields of view.
1
8
15
22
29
36
43
50
57
64
71
78
85
92
99
106
113
120
127
134
141
148
155
162
169
176
183
190
197
Distance between central camera and OoI (m)

Fig. S11. The maximum measurable heights up to 200 m away from the central camera for the straight (A) and angled (B) configuration with cameras spaced 10 m apart, with 10 to 180 m between the cameras and the OoI.

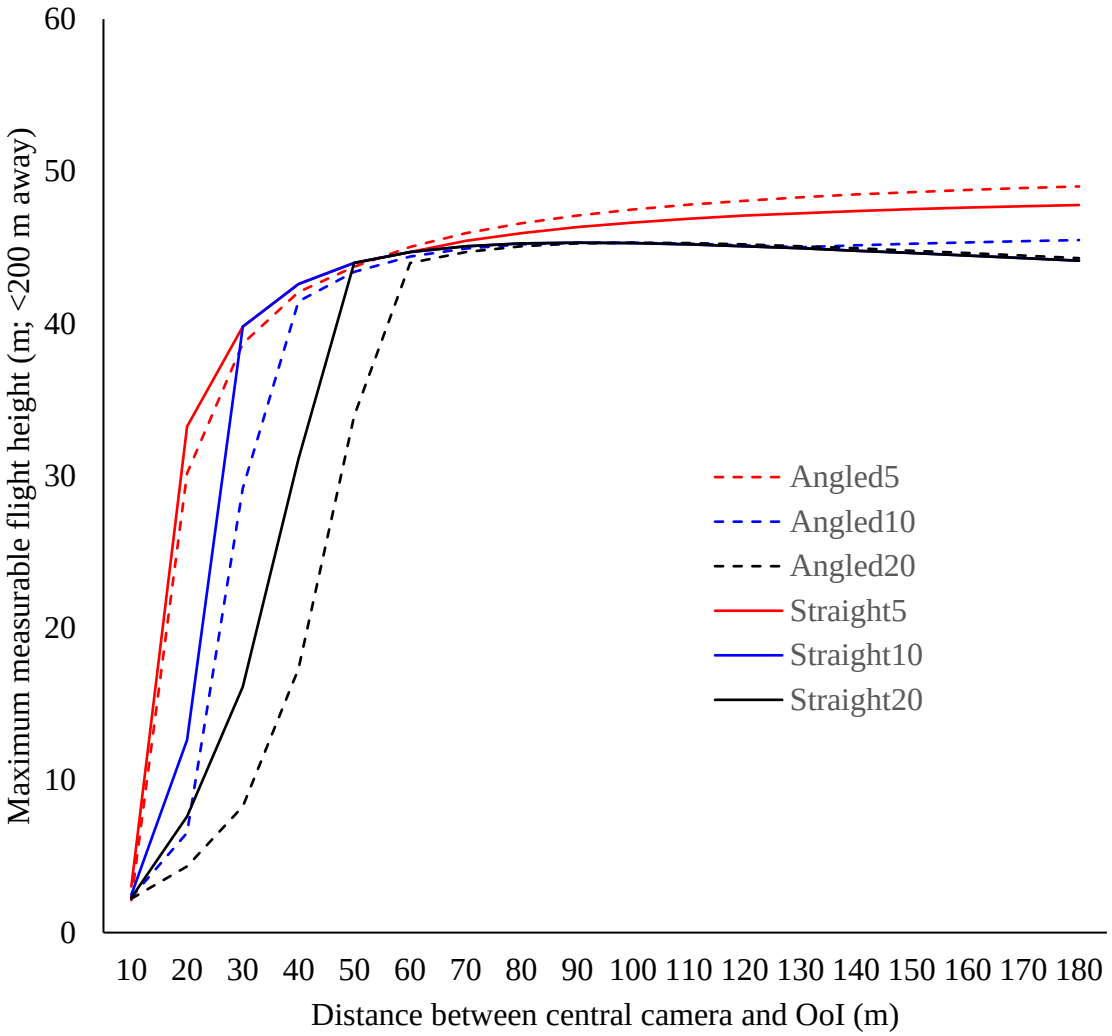

Fig. S12. Assuming flight heights can only be measured less than 200 m away from the central camera, these are the maximum flight heights for various configurations with the central camera varying in distance from the OoI.